3D background aerodynamics using CFD

Sørensen, Niels N.

Publication date:
2002

Document Version
Publisher's PDF, also known as Version of record

Risø-R-1376(EN)

3D Background Aerodynamics using CFD

Niels N. Sørensen

Risø National Laboratory, Roskilde, Denmark
November 2002

Abstract 3D rotor computations for the Greek Geovilogiki (GEO) 44 meter rotor equipped with 19 meters blades are performed. The lift and drag polars are extracted at five spanvise locations r/R= (.37, .55, .71, .82, .93) based on identification of stagnation points between 2D and 3D computations. The inner most sections shows clear evidence of 3D radial pumping, with increased lift compared to 2D values. In contrast to earlier investigated airfoils a very limited impact on the drag values are observed.

ISBN 87-550-3141-2
ISBN 87-550-3142-0(internet)
ISSN 0106-2840

Contents

1 Introduction *5*

2 Method *6*
2.1 Stagnation Point Location Method *6*
2.2 Direct Evaluation Using the Mean Axial Velocity *6*
2.3 Navier-Stokes Solver *7*

3 Geometry and computational mesh *9*
3.1 Surface generation *9*
3.2 Volume Mesh Generation *10*
3.3 Boundary Conditions *10*

4 Results *11*
4.1 Mechanical Power Production *11*
4.2 Lift and Drag polars *12*

5 Conclusion *15*

6 Acknowledgement *15*

1 Introduction

The DAMPBLADE project deals with the damping of wind turbine rotor blades from a structural point of view. The damping originating from the aerodynamics of the blades are therefore not the main focus of the project. Even though we do not focus on the aerodynamic damping, information of the aerodynamics of the blades are still needed to predict realistic loading on the blades.

There are several approaches for obtaining aerodynamic information for wind turbine blades. The most straightforward way is to directly measure the aerodynamics on a full scale rotor. Previous attempts have shown this to be both very complicated and very costly, additionally this attempt is very time consuming. Alternatively, wind tunnel measurements can be carried out for airfoil sections. This is again costly and do not give any information on the 3D effects present on a rotor in a rotational environment. Finally the possibility exists of using state of the art 3D Navier-Stokes rotor simulations to obtain the needed information. This approach is chosen here even though it is not without complications. One of the complications is the well known overestimation of the power production and loading in deep stall. In the present work the overestimation problem is controlled by comparing 3D computed values with corresponding 2D values. The methodology used to obtain the airfoil aerodynamics is described in the following, and the computed results are discussed.

2 Method

The method to determine the background aerodynamics for the GEO rotor is based on Navier-Stokes computations. In order to make the results from the Navier-Stokes rotor computations useful for the BEM computations applied for the stability computations in the DAMPBLADE project, the raw output of the rotor computations are transformed into lift and drag polar at five spanwise sections along the blade.

As the NS computations can be viewed as a numerical equivivalent of a real experiment, the extraction of lift and drag from the rotor computations poses some well know problems. The main problem is the determination of angles of attack. Previous studies has revealed that even for computations, where the amount of available data are orders of magnitude large than in an experiment, the determination of the angle of attack is not trivial. Several methods has previously been applied, using inverse Blade Element Momentum methods, stagnation point identification between 2- and 3D CFD computations etc. Previously the best results has been obtained using the stagnation point method that will be described in the following, but even this method is not without complications. One basic problem is the intend to identify a corresponding 2D angle of attack, even though it may be questionable whether these really exists. As the rotor enters the stalled region spanwise flow starts to develop. The individual airfoil sections therefore experiences a flow physics that are greatly changed from the simple 2D behavior. The identification of an equivivalent 2D angle of attack therefore is an artifact, as the flow physics do not correspond to any 2D flow behavior. The methods proposed in the following for determining the angles of attack, are designed to give the correct angles of attack in the range where the sectional rotor flow can be identified with 2D equivalent cases.

2.1 Stagnation Point Location Method

The method used for this was first used in the EC program JOR3-CT98-0208, VISCEL as reported in Sørensen [12] and [8]. For a given radial section on the 3D rotor the procedure is as follows: A 2D polar is computed for the airfoil section at conditions corresponding to the Reynolds number seen by the actual 3D section. From the 2D computations a curve connecting the location of the stagnation point with the angle of attack is constructed (SPL/AOA curve), see Figure 1. Determining the location of the stagnation points from the sectional 3D C_p curves, the SPL/AOA curve can be used to compute the equivivalent 2D angle of attack. As seen from Figure 1 showing the SPL/AOA curve for the r/R=0.55 section, this curve gives three possible AOA's for a region near Cl max, where the variation in circulation makes the stagnation point move back and forth. In this region comparison between 2D and 3D C_p and C_f curves are used to determine which of the three possible AOA's is the relevant angle of attack. Additionally assumptions of some degree of continuity of the computed lift/drag curves can be used in guiding the best choice.

2.2 Direct Evaluation Using the Mean Axial Velocity

As a consequence of the problem of identifying a unique angle of attack in the stalled region one alternative method was tested. This method is based directly on the averaged axial velocity in the rotor plane. By performing an averaging of

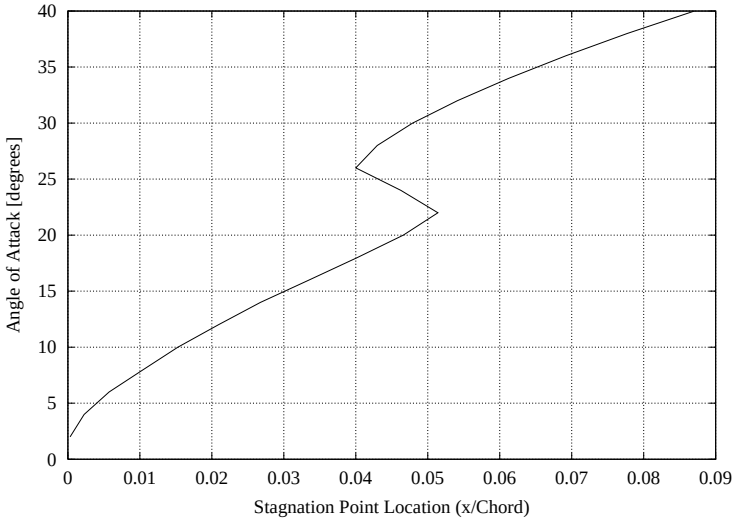

Figure 1. Curve connecting the 2D stagnation point location with the 2D angle of attack, for the r/R=0.55 section.

the axial velocity over a thin annulus $(r - \delta r, r + \delta r)$, at several axial positions it is possible to determine the mean axial velocity at the rotor disc. Using this axial velocity along with the rotational velocity, the angle of attack can be directly determined. Comparing the present method with the previous SPL method, small differences in the determined angles are observed. As the deviations are small, especially in the stalled region half a degree may not be very important, the direct evaluation of the axial velocity may be preferable. Unfortunately the determination of the averaged axial velocity at a given radius is very cumbersome.

2.3 Navier-Stokes Solver

The in-house flow solver EllipSys3D is used in all computations presented in the following. The code is developed in co-operation between the Department of Mechanical Engineering at DTU and The Department of Wind Energy at Risø National Laboratory, see Michelsen[2, 3] and Sørensen[7]. The EllipSys3D code is a multiblock finite volume discretization of the incompressible Reynolds Averaged Navier-Stokes (RANS) equations in general curvilinear coordinates. The code uses a collocated variable arrangement, and Rhie/Chow interpolation [6] is used to avoid odd/even pressure decoupling. As the code solves the incompressible flow equations, no equation of state exists for the pressure, and the SIMPLE algorithm of Patankar [13] is used to enforce the pressure/velocity coupling. The EllipSys3D code is parallelized with MPI for execution on distributed memory machines, using a non-overlapping domain decomposition technique. For rotor computations, a non-inertial reference frame attached to the rotor blades is used, and terms accounting for the Coriolis and centripetal forces are added to the momentum equations. Polar velocities (v_r, v_θ, v_z) are used in order to allow simple treatment of periodic boundary conditions in the azimuth direction, Michelsen[4] and Sørensen[9]. The solution is advanced in time using a 2nd order iterative time-stepping (or dual time-stepping) method. In each global time-step the equations are solved in an iterative manner, using underrelaxation. First, the momentum equations are used as a predictor to advance the solution in time. At this point in the computation the flowfield will not fulfill the continuity equation. The rewritten continuity equation (the so called pressure correction equation) is used as a correc-

tor making the predicted flowfield satisfy the continuity constraint. This two step procedure corresponds to a single sub-iteration, and the process is repeated until a convergent solution is obtained for the timestep. When a convergent solution is obtained, the variables are updated, and we continue with the next timestep.

For steady state computations, the global time-step is set to infinity and dual time stepping is not used, this corresponds to the use of local time stepping. In order to accelerate the overall algorithm, a three level grid sequence is used in the steady state computations. The convective terms are discretized using a second order upwind scheme, implemented using the deferred correction approach first suggested by Khosla and Rubine [5]. Central differences are used for the viscous terms, in each sub-iteration only the normal terms are treated fully implicit, while the terms from non-orthogonality and the variable viscosity terms are treated explicitly. Thus, when the sub-iteration process is finished all terms are evaluated at the new time level.

In the present work the turbulence in the boundary layer is modeled by the k-ω SST eddy viscosity model of Menter [11]. The details of the model will not be given here, we will only state that the model is chosen because of the very promising results for 2D separated flows, Wilcox[1] and Menter[10]. The equations for the turbulence model are solved after the momentum and pressure correction equations in every sub-iteration/pseudo time step. The three momentum equations are solved decoupled using a red/black Gauss-Seidel point solver. The solution of the Poisson system arising from the pressure correction equation is accelerated using a multigrid method.

3 Geometry and computational mesh

In order to perform the 3D CFD computations needed to obtain the background aerodynamics for the DAMPBLADE project, a computational mesh must first be constructed. There are several steps in this procedure and in the following the main steps will be described.

3.1 Surface generation

Based on the sectional description delivered by the three Greek partners, GEO, CRES and NTUA a digital surface geometry description was generated. To obtain a surface of sufficient quality for the CFD computations some processing of the original data provided was necessary, eliminating abrupt shifts in surface curvature, crossing trailing edges and closing open trailing edges. Additionally the outermost 20 cm of the 19 m blade were constructed based on photos using a NURBS surface generator, in order to resolve the double curved geometry, see Figure 2. For the main part of the blade inhouse RISOE software was used to construct a surface mesh based on the digitized surface, while the outermost 5 % of the blade near the tip where the surface is strongly double curved the MEGACADS program by DLR was used. The surface mesh has 256 cells in the chordwise direction, 64 cells in the spanwise direction, and one extra block to resolve the blade tip.

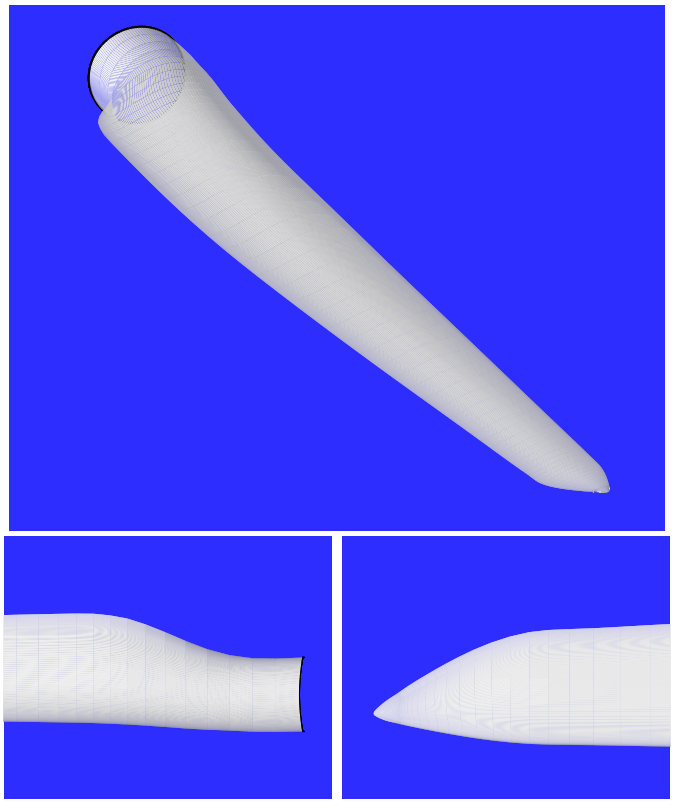

Figure 2. Geometry of the GEO blade showing a perspective view of the blade at the top, and the root and tip sections at the bottom of the figure

3.2 Volume Mesh Generation

Generating the volume mesh for the three bladed rotor, the 120 degrees periodicity of the rotor is exploited by only meshing one blade. The remaining two blades are included in the computations through the use of periodic boundary conditions. The volume mesh for the 120 degrees section is constructed in the following way. Based on the 5 block surface mesh, a O-O-mesh is constructed around the blade using the Risø HypGrid3D hyperbolic mesh generation code. The O-O-topology extends approximately 8 meters up and downstream of the rotor disc, and span 120 degrees in the rotation direction. The cell at the wall has a $y^+ \sim 2$ in order to resolve the boundary layer, and the points are distributed using a hyperbolic tangent function. To take the farfield boundary approximately 500 meters or 12 rotor diameters away from the rotor, an outer 3 block O-configuration was added on top of the inner O-O-configuration. The total mesh has around 2 million cells, see Figure 3.

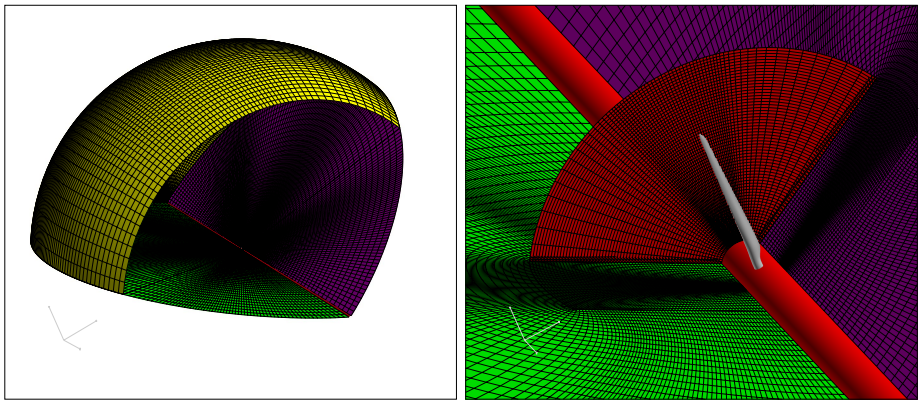

Figure 3. Volume mesh around the GEO rotor, the left picture shows one 120 degrees section,while the left figure shows details of the mesh near the rotational axis.

3.3 Boundary Conditions

The following boundary conditions are used in the computations. On the upstream part of the outer spherical part of the domain, the part of the outer boundary visible in Figure 3 the undisturbed velocity is specified. On the downstream part of the outer boundary fully developed conditions are assumed. On the inner cylindrical boundary along the rotational axis Euler/Slip conditions are specified, while no-slip conditions are specified on the blade of the surface. Finally fully implicit periodic conditions are specified on the two 120 degrees periodic planes.

4 Results

In the following the setup and results for the GEO 19 meters blade is described. The computed rotor has a diameter of 44 meters, and a rotational speed of 27 RPM. For the investigated case a 2 degree nose up (towards higher angles of attack) tip pitch is used. The originally planned 10 TSR's was supplemented by 3 additional TSR's to get a better representation of the flow around max power production. The simulated wind speeds are, 7, 10, 12, 13, 14, 15, 16, 17, 18, 19, 20, 22, 25 m/s. As agreed upon the computations were performed in stationary mode, computing towards a steady state situation. All computations were computed on the Risø IBM SP machine, on 330 Mhz Power3 processors, resulting in a computing time of 30 hours per wind speed using 4 processors. As previous described the EllipSys2D/3D codes were used for all computations presented in the following.

A long variety of results can be extracted from the 3D rotor computations, here we will concentrate on the mechanical power production, and the lift and drag coefficients at five spanwise positions. The five spanwise positions considered in the present work are r/R = (0.37, 0.55, 0.72, 0.81, 0.93).

4.1 Mechanical Power Production

First of all the computed mechanical power is shown along with the Nordtank 500/41 turbine power curve for reference, see Figure 4. As seen from the figure a very high maximum power is predicted. If we rely on previous experience from other rotors, we may expect a overprediction around 25-40 %. Based on this the maximum power would be around 610-760 kW for a wind speed of 18 m/s. Compared to the Nordtank rotor, the GEO power curve has a change in the slope at 10 m/s towards a larger increase in power. This may indicate that when stall begins to spread along the blade, 3D effects are more pronounced on the GEO blade than on the LM19.1 blade used on the Nordtank 500/41 rotor.

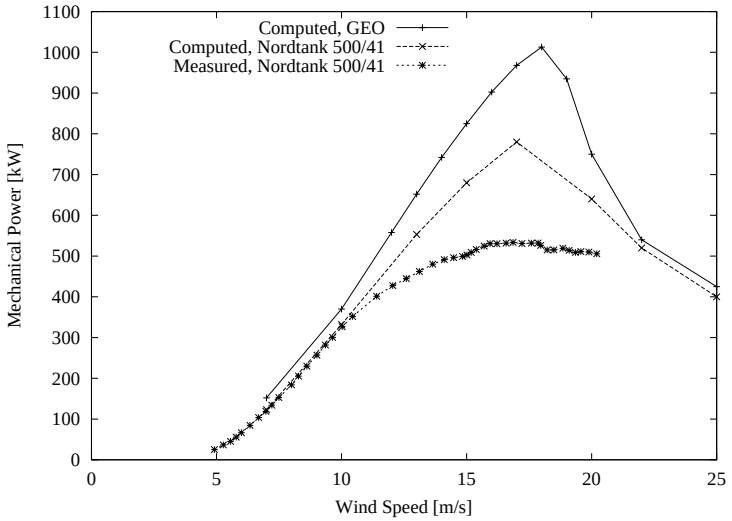

Figure 4. Comparison of computed mechanical power for the GEO rotor, the Nordtank 500/41 rotor and measurements of the Nordtank 500/41 rotor.

To illustrate that stall has actually spread to a large part of the blade at 10 m/s the suction side of the blade is shown in figure 5. In the separated area near the trailing edge, the spanwise flow component responsible for the radial pumping is

clearly visible.

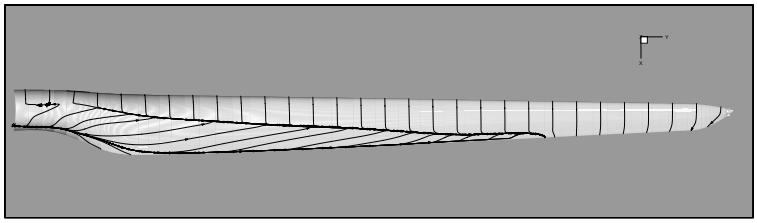

Figure 5. Limiting streamlines on the suction side of the GEO blade, for a wind speed of 10 m/s.

4.2 Lift and Drag polars

Based on the stagnation point location method (SPL method), the lift and drag polars are extracted at the five spanwise sections. The curves are given in figure 6 to 10. As expected from theory the lift is increased on the inboard stations as a consequence of the 3D effects caused by the radial pumping. Additionally it is observed that, as we move from the inboard station (r/R=0.37) towards the tip (r/R=0.93) the 3D lift curves gradually becomes closer to the 2D results. This is in good agreement with theory. It is observed that the increase in lift, is accompanied by an increase in drag for the inboard station (r/R=0.37). For the remaining stations the change in drag is very small, and in several cases a small decrease are observed, see figures 7 to 10. For a few cases the angles of attack were additionally determined directly using the averaged velocity at the respective radius in the rotor plane, see table 4.2, and good agreement was found for all cases considered.

Table 1. Comparison of angles of attack determined using the stagnation point method and directly using the induced velocity at the rotor plane.

Wind Speed [m/s]	r/R	AOA (SPL)	AOA (Direct)
7.0	0.81	6.44	6.78
14.0	0.37	21.34	19.83
14.0	0.55	18.20	17.89
14.0	0.72	15.80	15.86
14.0	0.81	14.75	14.99
14.0	0.93	12.10	13.64
19.0	0.81	21.03	20.79

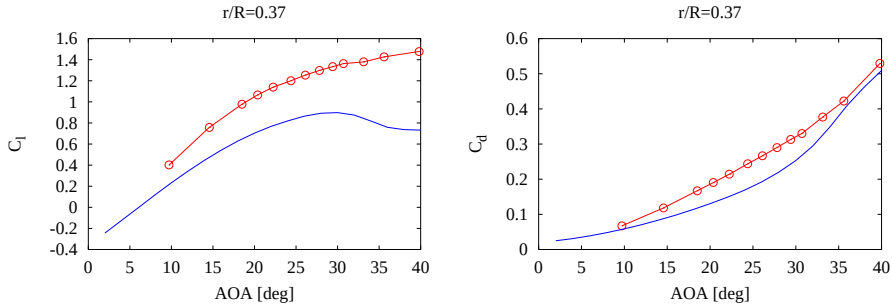

Figure 6. Lift and drag curve for the r/R=0.37 % section.

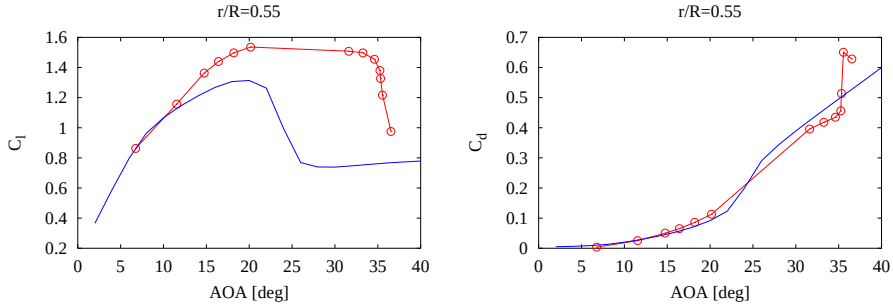

Figure 7. Lift and drag curve for the r/R=0.55 % section.

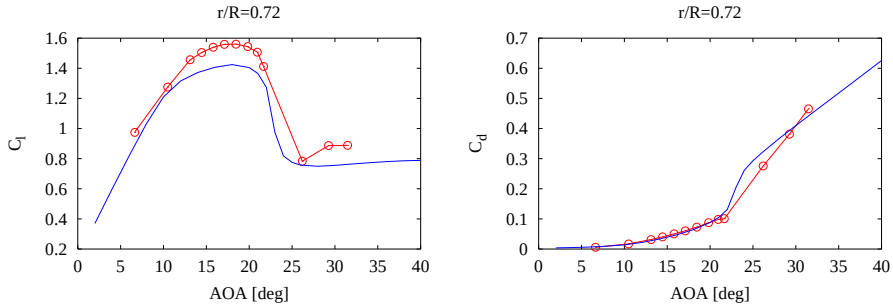

Figure 8. Lift and drag curve for the r/R=0.72 % section.

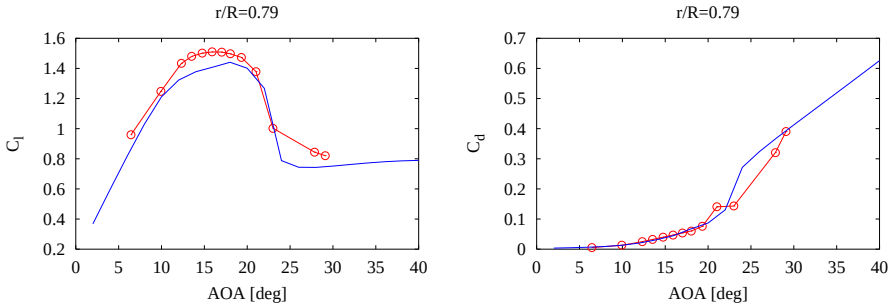

Figure 9. Lift and drag curve for the r/R=0.79 % section.

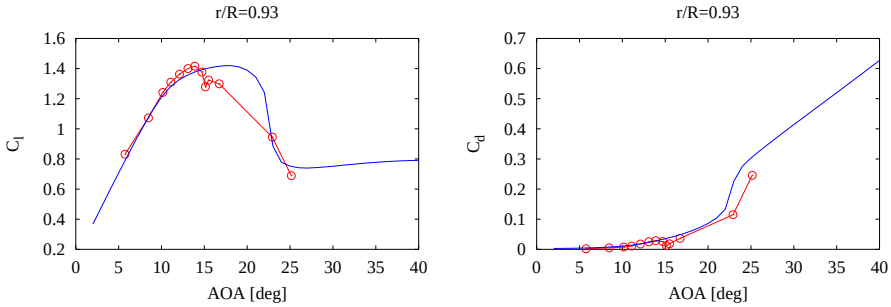

Figure 10. Lift and drag curve for the r/R=0.93 % section.

5 Conclusion

The background aerodynamics for a 44 meter rotor with the Geovilogiki 19 meter blade were computed for 13 wind speeds covering the normal operational range of the turbine. From the computations the angles of attack were determined by to different methods, namely the Stagnation Point Method using pressure distributions and directly by computing the velocity at the rotor disc. Based on the aerodynamic forces and the computed angle of attacks, lift and drag polars were extracted for five spanwise sections r/R=(0.37, 0.55, 0.72, 0.81, 0.93). The lift polars showed the theoretically expected rotational argumentation of the lift near the root of the blade. The rotational effect diminished outboard on the blade and the lift approached 2D values. Right at the tip and the values went below the 2D reference values. The influence on the profile drag was not very pronounced, and only at the innermost section a increased drag was observed.

6 Acknowledgement

The work was carried out under a contract with EC, ENK6-2000-00320, DAMP-BLADE. Computations were made possible by the use of the IBM RS6000 SP at the Risø central computing facility.

References

[1] Wilcox D. C. A Half Century Historical Review of the K-ω Model. AIAA-91-0615, 1991.

[2] Michelsen J.A. Basis3D - a Platform for Development of Multiblock PDE Solvers. Technical Report AFM 92-05, Technical University of Denmark, 1992.

[3] Michelsen J.A. Block structured Multigrid solution of 2D and 3D elliptic PDE's. Technical Report AFM 94-06, Technical University of Denmark, 1994.

[4] Michelsen J.A. General curvilinear transformation of the Navier-Stokes equations in a 3D polar rotating frame. Technical Report ET-AFM 98-01, Technical University of Denmark, 1998.

[5] Khosla P. K. and Rubin S. G. A diagonally dominant second-order accurate implicit scheme. *Computers Fluids*, 2:207–209, 1974.

[6] Rhie C. M. *A numerical study of the flow past an isolated airfoil with separation.* PhD thesis, Univ. of Illinois, Urbane-Champaign, 1981.

[7] Sørensen N. N. General Purpose Flow Solver Applied to Flow over Hills. Risø-R- 827-(EN), Risø National Laboratory, Roskilde, Denmark, June 1995.

[8] Sørensen N.N. Evaluation of 3D effects from 3D CFD computations. In *IEA Joint Action. Aerodynamics of wind turbines. 14th Symposium*, Boulder, CO, USA, December 2000.

[9] Sørensen N.N. and Michelsen J.A. Aerodynamic Predictions for the Unsteady Aerodynamics Experiment Phase-II Rotor at the National Renewable Energy Laboratory. AIAA Paper 2000-0037, 2000.

[10] Menter F. R. Performance of Popular Turbulence Models for Attached and Separated Adverse Pressure Gradient Flows. *AIAA Journal*, 30(8):2066–2072, August 1992.

[11] Menter F. R. Zonal Two Equation k-ω Turbulence Models for Aerodynamic Flows. AIAA-paper-932906, 1993.

[12] N.N Sørensen. Viscous and Aeroelastic Effects on Wind Turbine Blades, VISCEL. Task-2 report Contract JOR3-CT98-0208, European Commission, Nov. 2000.

[13] Patankar S. V. and Spalding D. B. A Calculation Prodedure for Heat, Mass and Momentum Transfer in Three-Dimensional Parabolic Flows. *Int. J. Heat Mass Transfer*, 15:1787, 1972.

Bibliographic Data Sheet **Risø-R-1376(EN)**

Title and author(s)

3D Background Aerodynamics using CFD

Niels N. Sørensen

ISBN	ISSN
87-550-3141-2 87-550-3142-0(internet)	0106-2840

Dept. or group	Date
Ris National Laboratory Wind Energy Department	Nov 2002

Groups own reg. number(s)	Project/contract No.
	1110031-00

Pages	Tables	Illustrations	References
18	1	11	12

Abstract (Max. 2000 char.)

3D rotor computations for the Greek Geovilogiki (GEO) 44 meter rotor equipped with 19 meters blades are performed. The lift and drag polars are extracted at five spanvise locations r/R= (.37, .55, .71, .82, .93) based on identification of stagnation points between 2D and 3D computations. The inner most sections shows clear evidence of 3D radial pumping, with increased lift compared to 2D values. In contrast to earlier investigated airfoils a very limited impact on the drag values are observed.

Descriptors INIS/EDB

AERODYNAMICS; AIRFOILS; COMPUTATIONAL FLUID DYNAMICS; FLOW MODELS; NAVIER-STOKES EQUATIONS; THREE-DIMENSIONAL CALCULATIONS; TWO-DIMENSIONAL CALCULATIONS; WIND TURBINES